2010 IEEE International Conference on Robotics and Automation
Anchorage Convention District
May 3-8, 2010, Anchorage, Alaska, USA

A Passive Weight Compensation Mechanism with a Non-Circular Pulley and a Spring

Gen Endo, Hiroya Yamada, Akira Yajima, Masaru Ogata and Shigeo Hirose

Abstract— **We propose a new weight compensation mechanism with a non-circular pulley and a spring. We show the basic principle and numerical design method to derive the shape of the non-circular pulley. After demonstration of the weight compensation for an inverted/ordinary pendulum system, we extend the same mechanism to a parallel five-bar linkage system, analyzing the required torques using transposed Jacobian matrices. Finally, we develop a three degree of freedom manipulator with relatively small output actuators and verified that the weight compensation mechanism significantly contributes to decrease static torques to keep the same posture within manipulator's work space.**

I. INTRODUCTION

A serial link arm with revolute joints requires large torque to compensate its own gravity especially for a base actuator due to serially connected linear configuration. Installing large actuators to generate compensation torque is not energy efficient because the actuator power is merely used to keep static balance and not used for external work. Moreover, using large actuators may lead to a negative spiral because large actuators are usually heavy and installing heavy actuators increases the total weight of the arm which consequently generates more gravity torque. Therefore a passive weight compensation mechanism is desirable to achieve high performance and high energy efficiency for various tasks.

Fig.1 shows typical examples of passive weight compensation mechanism for a one degree of freedom (DOF) inverted pendulum system. There is a spring between the base link and rotating arm link, and gravity torque depending on link posture θ is compensated by the spring force in Figs.1(a) (b). This simple mechanism is widely used for industrial robots to improve energy efficiency because it reduces maximum gravity torque. Additionally the spring-suspended configuration is also safer because the mechanism prevents the link from rapid falling in case of power shutdown. (Note that Fig.1(a) and (b) can be analyzed using the same kinematic model, however configuration in Fig.1(b) recently becomes more popular due to large workspace and small width of the robot.)

However, Fig.1(a)(b) with an ordinary linear spring can not perfectly compensate gravity torque within link's workspace. This is because the mechanism requires an ideal linear spring whose natural length is zero to compensate gravity torque regardless of the link posture θ [1]. To solve this problem, Rahman et al.[2] proposed a new configuration where a spring is installed within the link and the end of the spring is connected to the base link using a wire-pulley mechanism. This configuration virtually equals to the ideal spring (Fig.1(c)). (The same mechanism is also proposed by Morita et al. [3]) However a linear spring generating sufficient compensation force tends to be large and the material of the spring is usually heavy steel. Thus this mechanism may increase the total weight of the arm.

Fig.1(d) has a counter-weight at the end of the link to compensate the weight of the end effector. This mechanism can keep the center of gravity on the joint axis and thus moment of gravity force of the base link is always zero regardless of θ. This configuration is suitable for an application where the base link can not be rigidly fixed to the ground [4]. On the other hand, moment of inertia increases due to additional weight for counter balance. Therefore it is not appropriate for rapid movement with large acceleration and deceleration.

Based on the previous works, we decide to adopt the most popular configuration Fig.1(b) and propose to install a non-circular pulley rotating with arm link to perfectly balance within arm's workspace [5].

There are several former works to appropriately adjust spring force/torque profile by a non-circular pulley. Okada proposed a pantographic mechanism with non-circular pulleys and springs for an inner pipe inspection mobile robot to generate constant the pushing normal force of driving wheels against various diameter pipes [6]. Ulrich et al. developed a weight compensation mechanism with non-circular pulleys and parallel antagonistic linear springs for a serial link two DOF system. However, these previous works still remain laboratory experiment level because they required many assumptions to analytically derive the shape of the non-circular pulley, which is not preferable for practical design.

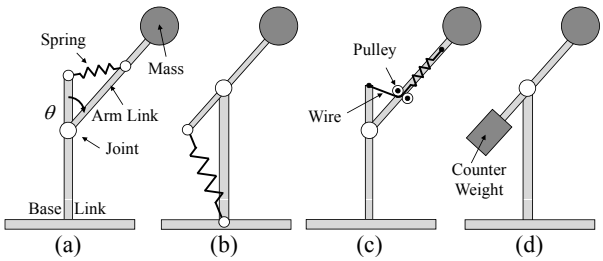

Fig. 1. Conventional weight compensation mechanism

G. Endo, H. Yamada and S. Hirose are with Dept. of Mechanical and Aerospace Engineering, Graduate School of Science and Engineering, Tokyo Institute of Technology, 2-12-1-I1-60 Ookayama, Meguro-ku, Tokyo 152-8552, Japan {gendo, hirose}@mes.titech.ac.jp

H. Yamada is with Grobal Edge Institute, Tokyo Institute of Technology, 2-12-1 Ookayama, Meguro-ku, Tokyo 152-8552, Japan yamada@robotics.mes.titech.ac.jp

A. Yajima and M. Ogata are with Canon Inc., 70-1 Yanagi-cho, Saiwai-ku, Kawasaki-shi, Kanagawa 212-8602, Japan

In this paper, we propose a numerical design method to derive the shape of the non-circular pulley which is more practical and applicable to the various industrial robots. We develop five-bar linkage parallel link arm with active joints and apply the weight compensation mechanism. We demonstrate that the weight compensation mechanism remarkably contributes to decrease static torques to keep the same posture within manipulator's workspace by hardware verifications.

In Section II, we explain basic principle of the weight compensation with a non-circular pulley and spring, and describe numerical design procedures for the non-circular pulley. Then we verify the effectiveness of the design with a passive one DOF pendulum system. In Section III, we extend the mechanism to two DOF five-bar parallel link system analyzing the gravity torques using transposed Jacobian matrices. We show that five-bar parallel link mechanism can be decomposed into two one DOF pendulum systems. In Section IV, we develop a five-bar parallel link arm with active joints with weight compensation mechanism and experimentally show that the proposed mechanism significantly decreases static torques to statically maintain the same posture in arm's workspace. Finally we conclude this paper and discuss future works in Section V.

II. Weight Compensation Mechanism with a Non-circular Pulley and a Spring

A. Basic Principle

In this section, we discuss the basic principle of the weight compensation mechanism for an one DOF pendulum system (Fig.2). The arm link with the end-mass freely rotates w.r.t the base link. The non-circular pulley is fixed to the arm link. One extremity of the spring is connected to the base link and the other extremity is connected to the flexible part without elongation such as a wire or a belt. The extremity of the flexible part is fixed to the pulley and the flexible part is twisted around the non-circular pulley. Therefore arm link rotation winds the flexible part and the stretched spring generates the compensation torque whose magnitude equals the spring force multiplied by the diameter of the non-circular pulley. We define $\theta = 0$ when the arm is perfectly inverted and define it as "inverted pendulum" ($0 \leq \theta \leq \pi/2$) or "ordinary pendulum" ($\pi/2 \leq \theta \leq \pi$) as a matter of convenience.

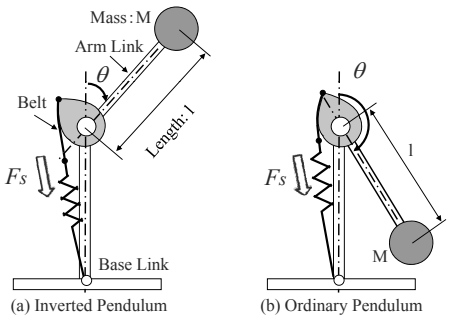

Fig. 2. Weight compensation mechanism with a non-circular pulley and a spring

If we can design pulley radius $r(\theta)$ satisfying the following identity, the system becomes totally balanced system with zero gravity.

$$F_s \cdot r(\theta) = Mgl\sin\theta, \tag{1}$$

where F_s is spring force and M, g, l are the weight of the end mass, gravity acceleration and link length, respectively.

This mechanism is composed of only three parts (non-circular pulley, flexible part and spring) and a very simple structure. Additional moment of inertia can be minimized using a high stiffness spring and a small diameter non-circular pulley. Moreover, we can set arbitrary torque profile $\tau(\theta)$ in the right-hand side of Eq.(1).

$$F_s \cdot r(\theta) = \tau(\theta). \tag{2}$$

We can set different torque profiles depending on the application. For example, "the arm generates lifting force of $mg/4$ when $\theta = \pi/2$". This means that the mechanism is not limited to the weight compensation only but is applicable to the various mechanism design.

In summary, this mechanism has the following advantages: 1) wide range and precise weight compensation, 2) minimum increase of moment of inertia, 3) arbitrary torque profile for various application.

B. Numerical design method for a non-circular pulley

In [7], two linear springs were arranged in parallel acting in an opposing manner to drive pulley. This configuration was introduced to mathematically derive the shape of the pulley. As a result, the total size of the mechanism was not compact enough for a practical application. In this paper, we derive the shape of the pulley by using the numerical iteration which is less constraining and more applicable compared with the previous symbolic approaches. The proposed algorithm is based on [8] which was used for adjusting the joint torque profiles using a Shape Memory Array (SMA) actuator. We extended the algorithm to set various torque profile[1]. The design procedure is as follows:

1) Set structural design parameters a, b in Fig.3, as well as initial arm angle θ_0 and desired torque profile $\tau(\theta)$.
2) Set spring stiffness k, natural length x_0, initial tension F_0. In case of an ordinary linear spring, spring force F_s can be expressed as $F_s = kx + F_0$, where x is the displacement.
3) Numerical design starts with the maximum displacement x_{max} of the spring, where initial pulley radius is $r_0 = \tau(\theta_0)/F_{max}$.
4) Draw a tangent line to the circle l_0 in order to intersect the fixed point of the spring P_0 in Fig.3, where the center of the circle is O and its radius is r_0. Define C_0 as the intersection of l_0 and X axis.
5) Draw a circle with radius of $\overline{OP_0}$ and define points $P_1, P_2, \ldots, P_n$ using a constant incremental angle $\Delta\theta$

[1]The shape of the non-circular pulley can be obtained by numerically solving an ordinary differential equations. However the graphical approach proposed here is less computational cost and provides the ease of intuitive understanding in trial-and-error process.

in the motion range ($\theta_0 \leq \theta \leq \theta_{max}$). This is because an analytical procedure is to be taken in which the pulley curve is drawn around the rotating center O by inversely rotating the spring supporting point P_i (instead of rotating the pulley) and unwinding the flexible part at the spring end from the pulley side.

6) Choose a random point α on the tangent line l_0. Obtain the displacement x_α of the spring stretched between the segment $\overline{\alpha P_1}$ and distance r_α of the straight line αP_1 from the origin O. The variation of the displacement of the spring stretched from the point α is $(\overline{\alpha P_0} - \overline{\alpha P_1})$ because the flexible part winding around the pulley is supposed to be non-ductile. Consequently, the displacement is $x_\alpha = x_{max} - (\overline{\alpha P_0} - \overline{\alpha P_1})$, where spring force is $F_{s\alpha} = k \cdot x_\alpha + F_0$.
7) Perform the operation in which the position of the point α is shifted until it agrees with the desired torque profile $\tau(\theta)$ by $F_{s\alpha} \cdot r_\alpha$ by means of a convergent calculation.
8) Make the position of α the point C_1, which is the first vertex of the pulley configuration to be polygonally approximated.
9) Assume a new point α on the straight line $\overline{C_1 P_1}$ and repeat the calculations of 6.- 8. for the points α and P_2 to obtain C_2.
10) Repeat the above-mentioned procedure until the displacement becomes zero or $\theta = \theta_{max}$.

In the above example, we select a linear spring with initial tension but we can select any kind of spring featuring non-linear properties. The numerical design proceeds in unwinding direction ($\Delta\theta \geq 0$) in this example but opposite winding direction ($\Delta\theta \leq 0$) is also possible. (Note that the initial displacement becomes minimum displacement in this case.)

This numerical method does not guarantee the convergence of the shape of the pulley. Thus, the pulley shape may diverge or converge to an extremely large radius depending on the initial parameter sets. On the other hand, this algorithm requires less constraints compared with symbolic methods and permits the designer to test various combination of springs and structural parameters which is appropriate for a practical design. The calculation time is less than $1sec$ with Intel Core2 Quad CPU 3GHz. Therefore we consider this algorithm as sufficiently practical method even if the designer has to search design parameters by trial and error.

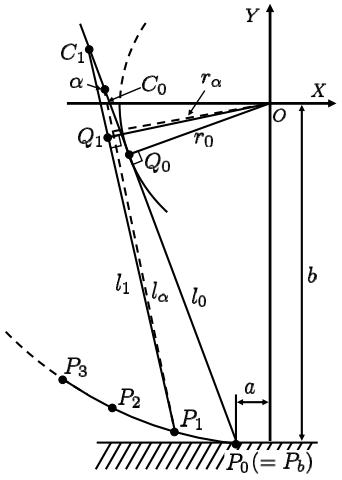

Fig. 3. Procedure to derive the non-circular pulley

C. Verification experiment for a one DOF pendulum system

To verify the proposed mechanism with numerical design method, we carry out weight compensation experiments for a one DOF inverted / ordinary pendulum shown in Fig.2. The non-circular pulley is designed on condition that the end mass is $0.5kg$, the length of the link is $0.5m$ and the diameter of the wire winded around the pulley is assumed to be negligible small. We choose a tension coil spring made of stainless steel (MISUMI Group Inc.: ACM12-100, $k = 1.15N/mm, F_0 = 14.71N, x_{max} = 75.21mm$). The weight compensated ranges of motion is maximized by manually adjusting structural parameters by trial and error. Derived non-circular pulleys for the inverted / ordinary pendulum are shown in Fig. 4, 5, respectively. The shape of the edges of the non-circular pulley which are not related to the weight compensation are arbitrary designed. The non-circular pulleys were manufactured by a CNC milling machine and the theoretical ranges of weight compensation are $18-90deg$ and $90-169deg$, respectively. The arm link can ideally keep any posture within these range of motion.

In case of an ordinary pendulum, the gravity torque is maximum at $\theta = \pi/2$ and gradually decreases as θ increases and finally becomes zero at $\theta = \pi$. Meanwhile the displacement of the spring is minimum at $\theta = \pi/2$ and gradually increases as θ increases and finally the spring force F_s becomes maximum at $\theta = \pi$. It is interesting that

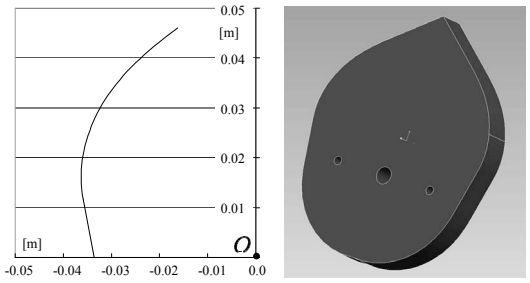

Fig. 4. Non-circular Pulley for an inverted pendulum

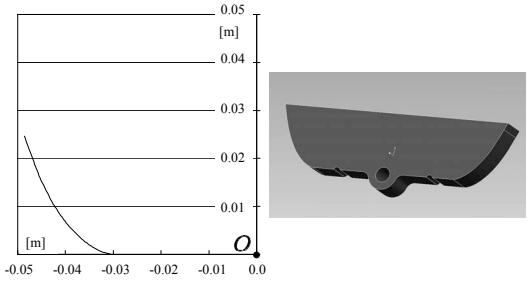

Fig. 5. Non-circular Pulley for an ordinary pendulum

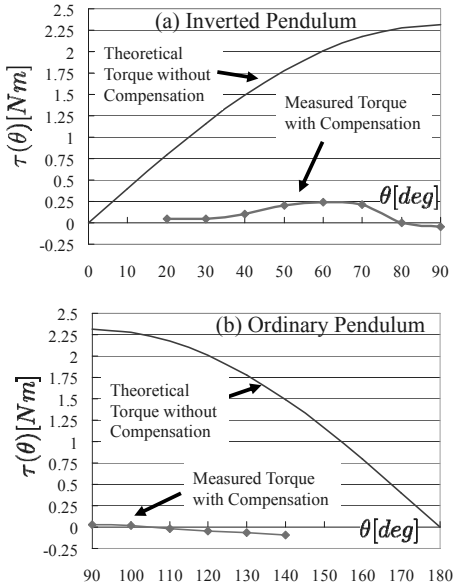

Fig. 6. Experimental results of weight compensation for a one DOF pendulum system

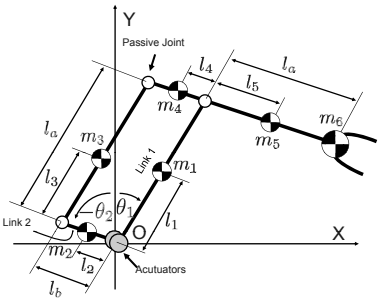

Fig. 7. Kinematic model of a parallel five-bar linkage arm with two DOF actuation

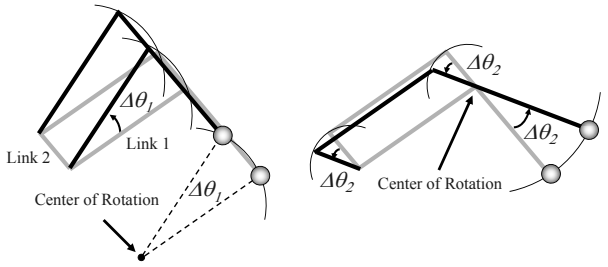

Fig. 8. Principle of virtual displacement for the parallel five-bar linkage

the proposed algorithm automatically solves this discrepancy by asymptotically making the pulley radius zero when θ approaches π so as to make $F_s \cdot r(\theta)$ zero.

Fig.6 illustrates joint torque measured by a spring balance. The arm could not always keep the same posture regardless of θ due to mechanical hardware error such as the elongation of wire, the effect of the diameter of the wire and deviation of spring stiffness. However Fig.6 clearly shows that the maximum joint torque with the weight compensation is less than 10 % of the theoretical gravity torque without weight compensation. [2]

III. Weight compensation for a two DOF five-bar linkage parallel link arm

In this section, we discuss the weight compensation mechanism for a two DOF five-bar parallel linkage arm shown in Fig.7. Two actuators are installed at the origin O and drive Link 1 and Link 2, independently. This configuration is often adopted by industrial robots because heavy actuators can be mounted on the base link that contributes to decrease moment of inertia of the arm. The question is whether the gravity torque for each joint is independent of each other.

Let us think about it using a principle of virtual displacement to intuitively understand the gravity torque acting on each joint (Fig.8). Suppose that Link 2 is fixed and only Link 1 slightly moves by $\Delta\theta_1$, the end mass rotates around rotation center indicated in Fig.8 left. Similarly, assuming that Link 1 is fixed and only Link 2 slightly moves by $\Delta\theta_2$, the end mass also rotates around the joint indicated in Fig.8 right. These results suggest that the displacement of the end mass due to θ_1 is independent from the movement of θ_2 and we can independently design a non-circular pulley for each joint.

To obtain symbolically gravity torques, the arm is modeled as a six-point-mass system including the weight of the links (Fig. 7). It is generally known that a joint torque vector τ can be obtained by external force vector $\mathbf{F}$ and transposed Jacobian matrix $\mathbf{J^T}(\theta)$ as follows.

$$\tau = \mathbf{J^T}(\theta)\mathbf{F} \tag{3}$$

The joint torque vector τ_i due to the point mass m_i is obtained by the inner product of the transposed Jacobian matrix $\mathbf{J_i^T}(\theta)$ for the position of m_i and the gravitational force vector considered as the external force $\mathbf{F_i} = (0, -m_i g)$. For example in the case of point mass m_6 located at the tip of the arm, its position vector p_6 and Jacobian matrix are expressed as follows:

$$p_6 = (l_a(\sin\theta_1 - \sin\theta_2),\ l_a(\cos\theta_1 - \cos\theta_2))^T, \tag{4}$$

$$\mathbf{J_6}(\theta) = \begin{pmatrix} l_a\cos\theta_1 & -l_a\cos\theta_2 \\ -l_a\sin\theta_1 & l_a\sin\theta_2 \end{pmatrix}. \tag{5}$$

Thus the joint torque vector $\tau_6 = (\tau_1^{(6)}, \tau_2^{(6)})^T$ is

$$\begin{pmatrix} \tau_1^{(6)} \\ \tau_2^{(6)} \end{pmatrix} = \begin{pmatrix} l_a\cos\theta_1 & -l_a\sin\theta_1 \\ -l_a\cos\theta_2 & l_a\sin\theta_2 \end{pmatrix} \begin{pmatrix} 0 \\ -m_6 g \end{pmatrix}, \tag{6}$$

$$\therefore \begin{pmatrix} \tau_1^{(6)} \\ \tau_2^{(6)} \end{pmatrix} = \begin{pmatrix} m_6 g l_a \sin\theta_1 \\ -m_6 g l_a \sin\theta_2 \end{pmatrix}. \tag{7}$$

By summing the joint torque vectors due to each mass point as $\tau = (\tau_1, \tau_2)^T = \sum_i \mathbf{J_i^T}(\theta)\mathbf{F_i}$, we obtain

$$\begin{pmatrix} \tau_1 \\ \tau_2 \end{pmatrix} = \begin{pmatrix} \{m_1 l_1 + m_3 l_3 + (m_4 + m_5 + m_6) l_a\} g \sin\theta_1 \\ \{m_2 l_2 + m_3 l_b + m_4 l_4 - m_5 l_5 - m_6 l_a\} g \sin\theta_2 \end{pmatrix}. \tag{8}$$

The Eq.(8) proves that τ_1 depends only on θ_1, and θ_2 never affects on τ_1, which is intuitively suggested by the principle of virtual work.

[2]The motion range of the ordinary pendulum was narrower than the intended due to the unexpected interference between arm link and base link or the pulley and the spring coil.

IV. Application to an actuated five-bar parallel link arm

A. Light duty light weight arm

We have developed a three DOF light weight arm for a pick & place task for an assembly of electric devices [10]. In this section, we describe outlines of the arm. We plan to report the detailed design and its specification in the next paper.

Fig. 9 and Table.I show the prototype and its specification of the developed arm. To span the three DOF polar coordinate system, a swivel joint is attached vertically to the base of the two DOF five-bar parallel link arm. The actuator output power is only $20W$ so as to permit a human worker to share the same working space with the arm. The developed arm is extremely light weight compared with a commercially available industrial robot with the same arm length such as [11](35kg).

B. Design of the weight compensation mechanism

The weight compensation torques for each joint are calculated by mass property data from 3D CAD model and Eqn.(8). The gravity torque for each joint can be come down to 1 DOF pendulum system model as mentioned before. The gravity torque τ_1 for J_1 is equivalent to an inverted pendulum with the end mass of $1.18kg$ and the link length of $0.5m$. Similarly, τ_2 is equivalent to an ordinary pendulum with $0.33kg$ and $0.5m$. τ_1 is much larger than τ_2 because of the longer link length.

Fig.10 shows derived shape of the non-circular pulleys based on mass property analysis. Theoretical ranges of the weight compensation in deg are $14.5 \leq \theta_1 \leq 90.0, -90.0 \leq \theta_2 \leq 0.0$. Two parallel springs are incorporated for J_1 compensation due to the high gravity torque. The specifications of the springs for J_1 and J_2 are ($x_0 = 100mm$, $k = 1.15N/mm$, $F_0 = 14.71N$, MISUMI Group Inc.: AUFM12-100) and ($x_0 = 80mm$, $k = 1.57N/mm$, $F_0 = 14.71N$, AUFM12-80), respectively.

To improve the accuracy of the weight compensation, we adopt a steel belt to connect the spring and a non-circular pulley instead of using a wire. The steel belt has $0.1mm$ thickness and negligible small elongation with sufficient strength.

J_1 and J_2 joint have the same driving mechanism. Fig.11 shows the detailed joint driving mechanism for J_1. The actuator output torque is transmitted by a timing-belt to the input shaft of the harmonic reduction gear unit. The output of the harmonic unit drives the non-circular pulley fixed to the link structure. The non-circular pulley winds the steal belt and stretch the spring to generate compensation torque. Note that the joint stiffness does not essentially decrease by introducing the spring because the spring is connected **parallel** to the joint actuation.

C. Experiment

To quantify the reduction of the joint torque to keep a static posture, we measure the absolute value of current for each actuator when the arm takes grid-points in $0.1m$ distance in absolute coordinate system. The torque is obtained by the actuator current and torque constant $43.8mNm/A$ of the actuator.

Fig.12 and Fig.13 indicate the torque difference of J_1 between without or with the weight compensation mechanism. Fig.14 and Fig.15 are comparison for J_2. The fan-shaped boundaries shows arm's workspace and contour lines are drawn by every $5mNm$. The maximum gravity torque for J_1, which has the longer link length, is $63.1mNm$ without the weight compensation mechanism (Fig. 12). Since the maximum continuous torque of the actuator described in the data

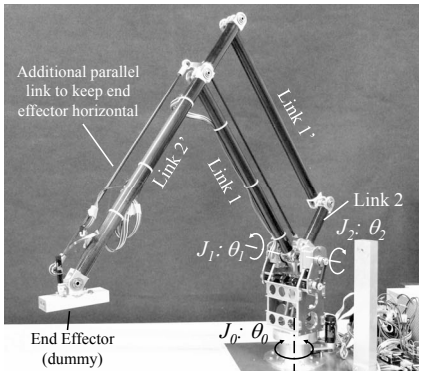

Fig. 9. Prototype of a parallel five-bar linkage arm for a light duty operation

TABLE I

Specification of the arm

Arm Length *mm*	500(Link 1)+500(Link 2')
Maximum Reach *mm*	R=985
Range of Motion *deg*	J_0: $\theta_0 = \pm 180$
	J_1: θ_1 = 0, 90 (where $\theta_1 - \theta_2 > 20$)
	J_2: θ_2 = -90, 0 (where $\theta_1 - \theta_2 < 160$)
Actuator	Maxon RE25 (20W) * 3
Payload *kg*	0.5
Total Weight *kg*	4.5

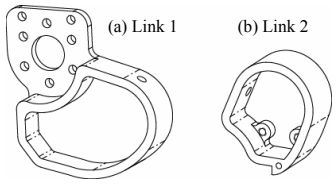

Fig. 10. Derived shape of the non-circular pulleys

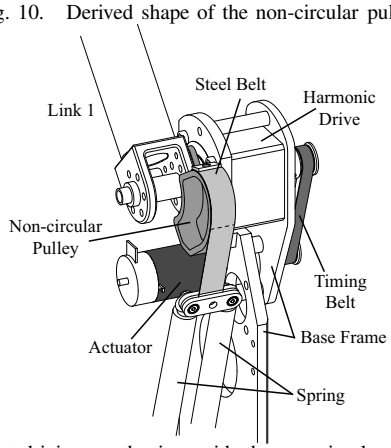

Fig. 11. Joint driving mechanism with the non-circular pulleys and the springs

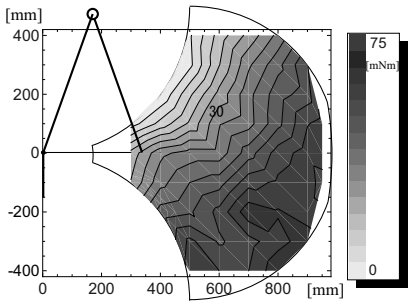

Fig. 12. τ_1 without compensation

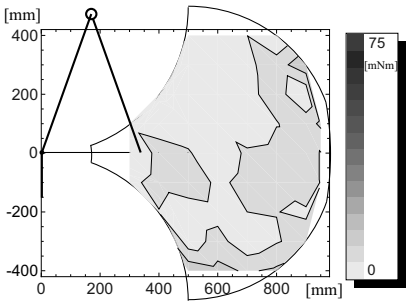

Fig. 13. τ_1 with compensation

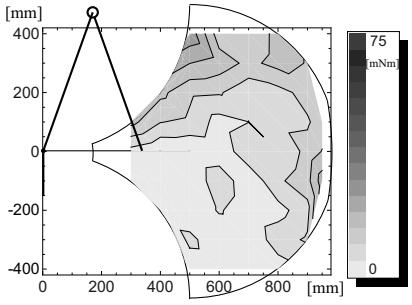

Fig. 14. τ_2 without compensation

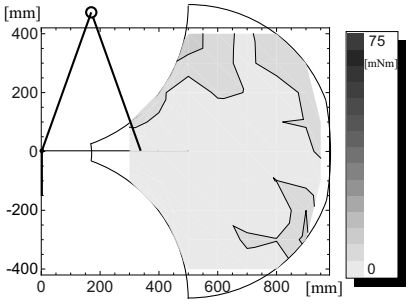

Fig. 15. τ_2 with compensation

sheet is only 28.4*mNm*, the installed actuator can statically sustain the posture less than in a half of the workspace. On the contrary with the weight compensation mechanism, required maximum torque is drastically decreased to 12.7*mNm* which is 80% off (Fig.13). Thus it is possible for the installed small actuator to sustain any posture within arm's workspace. In the same way, Fig.14 and Fig.15 show that the maximum torque on J_2 decreases from 26.3*mNm* to 12.4*mNm* which is 50% off. Therefore we could conclude that the proposed weight compensation mechanism is quite effective to reduce required torque to keep static posture with small actuators.

V. Conclusion

In this paper, we discuss a weight compensation mechanism with a non-circular pulley and a spring. We proposed a numerical design method to derive the shape of the pulley which is less constrained and more applicable compared to previous approaches. After preliminary verification of the design methodology for a single pendulum system, we extend the weight compensation mechanism to a two DOF parallel five-bar linkage arm, analyzing the gravity torques with transposed Jacobian matrices. The analysis reveals that the gravity torque for each joint can be come down to a one DOF pendulum system model. Finally we quantitatively investigate the effectiveness of the reduction of the required torque by measuring the actuator current of the light duty light weight arm. Introduction of the weight compensation mechanism significantly reduces the maximum static torque by 50-80% to sustain the same static posture.

In this paper, we present a new weight compensation method with a non-circular pulley and a spring. The comparison to the conventional weight compensation mechanisms will be interesting discussion. This paper focuses only on static balance and does not address an issue of stability in the dynamic movement. So far, we do not observe any negative effect such as diverging oscillation even in a rapid movement, dynamic effect should be discussed in the future works. Additionally, we determine the designing parameters for the non-circular pulley through a trial and error process and the shape of the non-circular pulley is not fully optimized yet. Using an optimization method also forms one of our future works.

References

[1] Herder J.L.: Energy-free systems: theory, conception and design of statically balanced spring mechanisms, http://repository.tudelft.nl/view/ir/uuid%3A8c4240fb-0315-462a-8b3b-efbd0f0e68b6

[2] Rahman T, Ramanathan R, Seliktar R, Harwin W: A simple technique to passively gravity-balance articulated mechanism, ASME Transactions on Mechanisms Design, 117(4): pp.655-658, 1995.

[3] Toshio Morita, Fumiyoshi Kuribara, Yuki Shiozawa, Shigeki Sugano: A Novel Mechanism Design for Gravity Compensation in Three Dimensional Space, *International Conference on Advanced Intelligent Mechatronics (AIM03)*, pp.163–168, 2003.

[4] Yuki Tojo, Paulo Debenest, Edwardo F. Fukushima, Shigeo Hirose: "Robotic System for Humanitarian Demining Development of Weight-Compensated Pantograph Manipulator", Proc. of Int. Conf. on Robotics and Automation, pp.2025-2030, 2004.

[5] Gen Endo, Shigeo Hirose: A Weight Compensation Mechanism with a Non-Circular Pulley and a Spring. Application to a Parallel Link Manipulator, *JSME Annual Conference on Robotics and Mechatronics*, 1A1-G20, 2008. (in Japanese)

[6] Tokuji Okada, Takeo Kanade: A Three-Wheeled Self-Adjusting Vehicle in a Pipe, FERRET-1, *International Journal of Robotics Research*, Vol.6, No.4, pp.60–75, 1987.

[7] Nathan Ulrich, Vijay Kumar: Passive Mechanical Gravity Compensation for Robot Manipulators, *Proc. of International Conference on Robotics and Automation*, pp.1536–1541, 1991.

[8] Shigeo Hirose, Koji Ikuta, Koichi Sato: Development of Shape Memory Alloy Actuator. Improvement of Output Performance by the Introduction of a σ-Mechanism, *Advanced Robotics*, Vol.3, No.2, pp.89–108, 1989.

[9] Japan Industrial Standards, JIS B 8433

[10] Gen Endo, Hiroya Yamada, Masaru Ogata, Shigeo Hirose: Development of a Light Duty Arm for a Cellular Manufacturing System, *The 26th Annual Conference of the Robotics Society of Japan*, 3A3-05, 2008. (in Japanese)

[11] http://www.denso-wave.com/en/robot/product/latest/vsg/index.html